01513/

AIAA 96-1716

On the Two Components of Turbulent Mixing Noise from Supersonic Jets

C. K. W. Tam and M. Golebiowski
Florida State University
Tallahassee, FL

J. M. Seiner
NASA Langley Research Center
Hampton, VA

2nd AIAA/CEAS Aeroacoustics Conference
May 6-8,1996/State College, PA

On the Two Components of Turbulent Mixing Noise from Supersonic Jets†

Christopher K.W. Tam* and Michel Golebiowski**
Florida State University
Tallahassee, FL 32306-3027

J.M. Seiner***
NASA Langley Research Center
Hampton, Virginia 23681

Abstract

It is argued that because of the lack of intrinsic length and time scales in the core part of the jet flow, the radiated noise spectrum of a high-speed jet should exhibit similarity. A careful analysis of all the axisymmetric supersonic jet noise spectra in the data-bank of the Jet Noise Laboratory of the NASA Langley Research Center has been carried out. Two similarity spectra, one for the noise from the large turbulence structures/instability waves of the jet flow, the other for the noise from the fine-scale turbulence, are identified. The two similarity spectra appear to be universal spectra for axisymmetric jets. They fit all the measured data including those from subsonic jets. Experimental evidence are presented showing that regardless of whether a jet is supersonic or subsonic the noise characteristics and generation mechanisms are the same. There is large turbulence structures/instability waves noise from subsonic jets. This noise component can be seen prominently inside the cone of silence of the fine-scale turbulence noise near the jet axis. For imperfectly expanded supersonic jets, a shock cell structure is formed inside the jet plume. Measured spectra are provided to demonstrate that the presence of a shock cell structure has little effect on the radiated turbulent mixing noise. The shape of the noise spectrum as well as the noise intensity remain practically the same as those of a fully expanded jet. However, for jets undergoing strong screeching, there is broadband noise amplification for both turbulent mixing noise components. It is discovered through a pilot study of the noise spectrum of rectangular and elliptic supersonic jets that the turbulent mixing noise of these jets is also made up of the same two noise components found in axisymmetric jets. The spectrum of each individual noise component also fits the corresponding similarity spectrum of axisymmetric jets.

Nomenclature

A = amplitude of the large turbulence structures/ instability waves noise

a_∞ = ambient sound speed

B = amplitude of the fine-scale turbulence noise

D = nozzle exit diameter

D_j = fully expanded diameter of a jet

f = frequency

f_F = frequency at the peak of the fine-scale turbulence noise spectrum

f_L = frequency at the peak of the large turbulence structures/instability waves noise spectrum

F = spectrum function of the large turbulence structures/instability waves noise

G = spectrum function of the fine-scale turbulence noise

M_c = convective Mach number

M_d = nozzle design Mach number

M_j = fully expanded jet Mach number

p_{ref} = reference pressure for the decibel scale $\left(2 \times 10^{-5} \frac{N}{m^2}\right)$

r = radial distance measured from the nozzle exit

S = sound power spectrum in dB per 1 Hz band

$\text{St} = \frac{fD}{V_j}$, Strouhal number

T_r = reservoir temperature

T_∞ = ambient temperature

V_j = fully expanded jet velocity

χ = inlet angle

* Professor, Department of Mathematics, Associate Fellow AIAA.

** Visiting Scholar.

*** Senior Research Scientist, Fluid Mechanics and Acoustics Division, Associate Fellow AIAA.

1. Introduction

It has been suggested by a number of investigators[1-3] that turbulent mixing noise from supersonic jets actually consists of two distinct components. One component is produced by the large turbulence structures/instability waves of the jet flow. The mechanism by which this component of noise is generated has been discussed in detail by Tam and Burton[4]. Basically, when the large turbulence structures/instability waves propagate downstream at supersonic speed relative to the ambient condition, Mach waves are generated; very much analogous to the Mach waves generated by supersonic flow over a wavy wall. This form of noise radiation has come to be known as Mach wave radiation. The second component of turbulent mixing noise is generated by the fine-scale turbulence of the jet. Although it is clear that turbulence would lead to flow unsteadiness and hence sound generation, yet the exact process by which fine-scale turbulence produces noise remains not well understood.

Figure 1 shows the measured noise directivities[5] at selected Strouhal numbers of a Mach 2 perfectly expanded jet. It was suggested by Tam and Chen[1] that the dominant part of the radiated noise (for figure 1, this corresponds to noise radiated in the downstream direction in the sector with inlet angle, χ, larger than 125 deg) was generated by the large turbulence structures/instability waves. They developed a stochastic instability wave model to predict this noise component. Their predicted results agreed well with the measured data. Seiner, Bhat and Ponton[6] carried out independent comparisons between instability wave calculations and experimental measurements. They reported that many prominent features of the dominant part of the radiated jet noise were consistent with instability wave predictions.

Tam and Chen[1] observed that for inlet angle, χ, less than 110 deg (see figure 1) the jet noise radiation was almost uniform without a strongly preferred direction. They suggested that this low-level, almost uniform background noise, was generated by the fine-scale turbulence of the jet flow. In other words, the fine-scale turbulence noise is dominant over inlet angles smaller than 110 deg for the experiment of figure 1. By implication in the intervening angular directions 110 deg $< \chi <$ 125 deg, both noise components are of equal importance. However, thus far, no experimental or theoretical results have been offered to substantiate their suggestion concerning the fine-scale turbulence noise.

The primary motivation of the present investigation is to offer irrefutable experimental evidence that turbulent mixing noise from high-speed axisymmetric jets, indeed, consists of two independent components possessing directivity characteristics consistent with the suggestion of Tam and Chen. As the investigation proceeded, other equally important issues, such as the effects of the presence of a shock cell structure in the jet plume and the jet Mach number effects (including subsonic Mach number) on the characteristics of the two noise components, were also studied. Below is a list of the objectives of the present study.

1. To provide concrete experimental evidence that turbulent mixing noise from supersonic jets is made up of two distinct components. Determination of the spectral and directivity characteristics of the two noise components as well as their relative importance is part of the research objective.
2. To investigate the effects of the presence of a shock cell structure in the jet plume on turbulent mixing noise.
3. To find if there are distinct qualitative differences/similarities between the turbulent mixing noise of supersonic and subsonic jets. Are their noise generation mechanisms the same?
4. To examine whether there are spectral similarities between turbulent mixing noise from nonaxisymmetric jets, specifically rectangular and elliptic jets, and axisymmetric jets.

To accomplish the above objectives, a careful study and analysis of all the axisymmetric jet noise spectral data (1,900 spectra in all), as well as some nonaxisymmetric jet noise spectra measured in the Jet Noise Laboratory of the NASA Langley Research Center was carried out. Details of the anechoic chamber and microphone array used in the measurements have been reported in Ref. [5] and will not be repeated here. Four axisymmetric nozzles were employed in the experiments. The dimensions and characteristics of these nozzles are given in Table 1. As can be seen from this table, this investigation concentrates on turbulent mixing noise data in the jet Mach number, M_j, range of 1.37 to 2.24 and temperature ratio ($\frac{T_r}{T_\infty}$) range from 1.0 to 4.9.

All the noise spectra used in the present study are narrow-band data in 122 Hz band. They are scaled to a distance of $100D_j$ where D_j is the fully expanded jet diameter[3]. D_j may be calculated by

the formula

$$D_j = D\left[\frac{1+(\gamma-1)\frac{M_j^2}{2}}{1+(\gamma-1)\frac{M_d^2}{2}}\right]^{\frac{\gamma+1}{4(\gamma-1)}}\left(\frac{M_d}{M_j}\right)^{\frac{1}{2}}.$$

We are aware that, in addition to the NASA Langley data, high-quality turbulent mixing noise from nearly perfectly expanded supersonic jets are also available in the published works of Yu[7], Yu and Dosanjh[8], Norum and Seiner[9] and Tanna[10]. The measurements of Tanna include high-temperature jets as well as cold jets. However, all these early data were measured in one-third octave band. They are well-suited for engineering applications. For our study, data with good frequency resolution are necessary and critical to its success. For this reason, the data of Ref. [7] to [10] were not used in the data analysis of this investigation.

2. Similarity Spectra

In the mixing layer of a turbulent jet there is no inherent geometrical length scale. Also, it is well-known that at high Reynolds number, viscosity is not a relevant parameter of turbulent jet flows. Based on these observations, it is easy to see that there is no intrinsic length and time scales in the core region of the jet flows. As a result, the mean flow as well as all the turbulence statistics of the flow must exhibit self-similarity. Over the years, that the mean flow of a high-speed turbulent jet possesses a similarity profile has been well-verified experimentally[11-14]. Extensive computations by Tam and Chen[1] in their stochastic instability wave model work have indicated that the dominant part of Mach wave radiation is generated in the core region of the jet. As will be discussed later, there is also strong evidence that the dominant part of fine-scale turbulence noise is generated in the core region of the jet where similarity prevails. The above facts and reasonings strongly suggest that the noise spectra of the two independent turbulent mixing noise components should also exhibit similarity. In the absence of an intrinsic time or frequency scale, the frequency f must be scaled by f_L, the frequency at the peak of the large turbulence structures/instability waves noise spectrum, or f_F which is the frequency at the peak of the fine-scale turbulence noise spectrum.

The noise of a high-speed jet naturally depends on the jet operating parameters V_j, T_r and D_j, the ambient condition, T_∞, the direction of radiation, χ, and the distance of the measurement point from the nozzle exit, r. On accounting for the contributions of the two independent noise components, the jet noise spectrum, S, may be expressed in the following similarity form,

$$S = \left[AF\left(\frac{f}{f_L}\right) + BG\left(\frac{f}{f_F}\right)\right]\left(\frac{D_j}{r}\right)^2 \qquad (1)$$

where $F(\frac{f}{f_L})$ and $G(\frac{f}{f_F})$ are the similarity spectra of the large turbulence structures/instability waves noise and the fine-scale turbulence noise. These spectrum functions are normalized such that $F(1) = G(1) = 1$. In (1), A and B are the amplitudes of the independent spectra; they have the same dimensions as S. The amplitudes A and B and the peak frequencies f_L and f_F are functions of the jet operating parameters, $\frac{V_j}{a_\infty}$ and $\frac{T_r}{T_\infty}$ and inlet angle χ.

In decibel form, (1) may be rewritten as,

$$10\log\left(\frac{S}{p_{\text{ref}}^2}\right) = 10\log\left[\frac{A}{p_{\text{ref}}^2}F\left(\frac{f}{f_L}\right) + \frac{B}{p_{\text{ref}}^2}G\left(\frac{f}{f_F}\right)\right] - 20\log\left(\frac{r}{D_j}\right) \qquad (2)$$

where p_{ref} is the reference pressure ($2 \times 20^{-5}\frac{N}{m^2}$) of the decibel scale. In the downstream directions, where the large turbulence structures/instability waves noise dominates, (2) simplifies to,

$$10\log\left(\frac{S}{p_{\text{ref}}^2}\right) = 10\log\left(\frac{A}{p_{\text{ref}}^2}\right) + 10\log F\left(\frac{f}{f_L}\right) - 20\log\left(\frac{r}{D_j}\right). \qquad (3)$$

Similarly, in the upstream directions, where the fine-scale turbulence noise dominates, (2) simplifies to,

$$10\log\left(\frac{S}{p_{\text{ref}}^2}\right) = 10\log\left(\frac{B}{p_{\text{ref}}^2}\right) + 10\log G\left(\frac{f}{f_F}\right) - 20\log\left(\frac{r}{D_j}\right). \qquad (4)$$

It is worthwhile to point out, if, indeed, (2) is valid, then the two similarity spectrum functions $F(\frac{f}{f_L})$ and $G(\frac{f}{f_F})$ have to be applicable to noise from an axisymmetric jet radiated in any direction χ regardless of the jet Mach number M_j and the jet to ambient temperature ratio $\frac{T_r}{T_\infty}$.

In the present investigation, the two similarity spectrum functions were initially determined empirically using a selected set of experimental data. Once found, they were checked by comparing with the entire data-bank at our disposal (1,900 spectra in all).

They fitted all the measured spectra over the entire range of Mach number and temperature ratio of the NASA Langley data.

Figure 2 shows the shape of the empirically determined spectrum functions in dB scale versus $\log(\frac{f}{f_{peak}})$ where $f_{peak} = f_L$ for the large turbulence structures/instability waves noise and $f_{peak} = f_F$ for the fine-scale turbulence noise. (Note: In a $\log(\frac{f}{f_{peak}})$ plot, the graph of $10\log F$ should fit the entire measured spectrum, if it is dominated by the large turbulence structure/instability waves noise, when the peak of the graph is put on top of the peak of the measured spectrum. The same is true for the fine-scale turbulence noise.) The two spectrum shapes are distinctly different. The $10\log F$ function has a relatively sharp peak and drops off linearly as shown. The $10\log G$ function, on the other hand, consists of a very broad peak and rolls off extremely gradually. For future reference and for convenience of application we have fitted these functions by simple piecewise continuous analytic functions. The analytic forms of these spectrum functions are:

$$10\log F = \text{(dB)} \begin{cases} 5.64174 - 27.7472\log\left(\frac{f}{f_L}\right); & \frac{f}{f_L} \geq 2.5 \\ \left[1.06617 - 45.29940\log\left(\frac{f}{f_L}\right) \right. & \\ \quad \left. +21.40972\left(\log\left(\frac{f}{f_L}\right)\right)^2\right] & \\ \quad \cdot\log\left(\frac{f}{f_L}\right); & 2.5 \geq \frac{f}{f_L} \geq 1 \\ -38.19338\left(\log\left(\frac{f}{f_L}\right)\right)^2 & \\ \quad -16.91175\left(\log\left(\frac{f}{f_L}\right)\right)^3; & 1 \geq \frac{f}{f_L} \geq 0.5 \\ 2.53895 + 18.4\log\left(\frac{f}{f_L}\right); & 0.5 \geq \frac{f}{f_F} \end{cases} \quad (5)$$

$$10\log G = \text{(dB)} \begin{cases} 29.77786 - 38.16739\log\left(\frac{f}{f_F}\right); & \frac{f}{f_F} \geq 30 \\ -11.8 - \left[27.2523 \right. & \\ \quad +0.8091863\log\left(\frac{f}{f_F}\right) & \\ \quad \left. +14.851964\left[\log\left(\frac{f}{f_F}\right)\right]^2\right] & \\ \quad \cdot\log\left(\frac{f}{f_F}\right); & 30 \geq \frac{f}{f_F} \geq 10 \\ -\left[8.1476823 \right. & \\ \quad \left. +3.6523177\log\left(\frac{f}{f_F}\right)\right] & \\ \quad \cdot\left[\log\left(\frac{f}{f_F}\right)\right]^2; & 10 \geq \frac{f}{f_F} \geq 1.0 \\ \left[-1.0550362 \right. & \\ \quad \left. +4.9774046\log\left(\frac{f}{f_F}\right)\right] & \\ \quad \cdot\left[\log\left(\frac{f}{f_F}\right)\right]^2; & 1.0 \geq \frac{f}{f_F} \geq 0.15 \\ -3.5 + \left[11.874876 \right. & \\ \quad +2.1202444\log\left(\frac{20f}{3f_F}\right) & \\ \quad \left. +7.5211814\left(\log\frac{20f}{3f_F}\right)^2\right] & \\ \quad \cdot\log\left(\frac{20f}{3f_F}\right); & 0.15 \geq \frac{f}{f_F} \geq 0.05 \\ 9.9 + 14.91126\log\left(\frac{f}{f_F}\right); & 0.05 \geq \frac{f}{f_F} \end{cases} \quad (6)$$

Figure 3 shows typically how well the spectrum function $10\log F$ fits the measured data. In making these comparisons, the maximum point of the $10\log F$ versus $\log(\frac{f}{f_L})$ graph, figure 2, is placed so that it coincides with the peak of the measured spectrum. In these examples, the jet Mach numbers are 1.5 and 2.0. The jet to ambient temperature ratio increases from 1.11 to 4.89. The direction of radiation, χ, varies from 138 deg to 160.1 deg. As can be seen, there is good agreement in all the cases. At very high frequencies, the agreement is less good in some cases. At this time, it is not clear what is the cause of this discrepancy. Figure 4 illustrates typical comparisons between the spectrum function $10\log G$ and measured data for perfectly expanded supersonic jets at $M_j = 1.5$ and 2.0 in directions for which the noise from fine-scale turbulence dominates. The jet to ambient temperature ratio covers the range of 0.98 to 4.89. The inlet angle χ, varies from 83.3 deg to 120.2 deg. Clearly, there is good agreement over the entire measured frequency range.

For angular directions neither too far upstream nor downstream both mixing noise components are important. In these cases, equation (2) must be used. Figure 5 shows examples of how the two noise spectra can be added together to reproduce the measured spectra. To obtain a good fit to the data, the amplitude functions A and B as well as the peak frequencies f_L and f_F are adjusted in each case. The separate contributions from each of the two noise components are shown in the figure.

We would like to note one important fact pointed out by figures 3, 4 and 5 is, both the large turbulence structures/instability waves noise and the fine-scale turbulence noise make significant contributions to the total noise of the jet over almost identical frequency range. That is, in terms of the total noise of the jet, both noise components are important over nearly all frequencies. This seems to contradict directly the traditional belief that large-scale turbulence generates mainly low frequency noise whereas high frequency noise comes primarily from fine-scale turbulence.

3. Characteristics and Relative Importance of the Two Noise Components

A good deal of the effort of the present investigation was spent to identify the jet operating parameters that would give the best correlation of the noise data. What we found was that the data could best be collapsed by using the parameter $\frac{V_j}{a_\infty}$ and $\frac{T_r}{T_\infty}$. We had tried to use M_j, the fully expanded jet Mach

number. But our experience had been that M_j was not as effective a parameter as $\frac{V_j}{a_\infty}$. We wish to mention that for broadband shock associated noise, M_j is a vital parameter for noise prediction[15-17]. In the shock noise problem, the shock strength is characterized by the parameter $(M_j^2-M_d^2)^2/(1+\frac{\gamma-1}{2}M_d)^2$. The intensity of the instability waves shock cell interaction, which generates the noise, is generally characterized by $M_j^2/(1+\frac{\gamma-1}{2}M_j^2)$ times the shock cell strength. We believe that M_j is an important parameter of broadband shock noise because it is critical to the shock cells (e.g. if M_j is less than 1, there would be no shock cells and hence no shock noise). The noise generation mechanisms of turbulent mixing noise are very different. They have nothing to do with shock cells in the jet plume. This being the case, the finding that M_j is not an effective correlation parameter for turbulent mixing noise should not be a surprise.

In decibel scale, the directional dependence of the large turbulence structures/instability waves noise amplitude turns out to be quite simple. A typical case is given in figure 6. Here SPL is effectively $10\log(A/p_{\text{ref}}^2) - 40$ dB. This quantity increases linearly with χ until a plateau is reached where the noise amplitude is practically constant. In the plateau region, the noise intensity is maximum. This maximum intensity is a function of the jet operating parameters, $\frac{V_j}{a_\infty}$ and $\frac{T_r}{T_\infty}$. Figure 7 shows a typical dependence of the amplitude of the fine-scale turbulence noise, $10\log(B/p_{\text{ref}}^2) - 40$ dB, on directivity. Again there is a linear increase with χ. The slope of the straightline relationship is a function of the jet operating parameters.

To obtain an idea of how the intensity of the large-scale turbulence structures/instability waves noise changes with jet velocity and temperature, we concentrate our attention on the maximum amplitude region of figure 6. In all the experimental conditions we have examined, $\chi = 160°$ is always in this region. We note also there is negligible contribution of fine-scale turbulence noise in this direction. Figure 8 is a plot of $10\log S$ versus $\log(\frac{V_j}{a_\infty})$ with $\frac{T_r}{T_\infty}$ as a parameter at $\chi = 160\,\text{deg}$ and $\frac{r}{D_j} = 100$. One obvious feature of this figure is that data correspond to the same jet to ambient temperature ratio align themselves along parallel straightlines. A good fit to the entire set of data is (in dB per 1 Hz band)

$$10\log\left(\frac{A}{p_{\text{ref}}^2}\right) = 75 + \frac{46}{(\frac{T_r}{T_\infty})^{0.3}} + 10\log\left(\frac{V_j}{a_\infty}\right)^n \quad (7)$$

where

$$n = 10.06 - 0.495\frac{T_r}{T_\infty}. \quad (8)$$

The exponent n is usually referred to as velocity exponent in jet noise literature. This velocity exponent is weakly dependent on jet temperature. For cold jets, n is approximately equal to 9.5 which is significantly larger than 3, a value believed by some to be appropriate for the overall sound pressure level of supersonic jets. On comparing with the so-called V_j^8 law, a result of the traditional Acoustic Analogy Theory, the exponent is still quite large. The main effect of temperature is given by the second term on the right side of equation (7). If the jet velocity is kept fixed, the peak noise level of the large turbulence structures/instability waves noise is less for hotter jets. As a point of reference, it is worthwhile to note that a jet with a temperature ratio of 2 is about 8.6 dB quieter than a cold jet in the direction of maximum noise intensity.

To assess the effect of jet operating conditions on the fine-scale turbulence noise, we concentrate on the noise radiated at $\chi = 90\,\text{deg}$. In this direction, there is practically no large turbulence structures/instability waves noise. Figure 9 shows a plot of $10\log S$ versus $\log(\frac{V_j}{a_\infty})$ with $\frac{T_r}{T_\infty}$ as a parameter at $\frac{r}{D_j} = 100$. Again the data corresponding to different jet temperature ratio can be adequately approximated by straightlines. A good fit to the data is (in dB per 1 Hz band),

$$10\log\left(\frac{B}{p_{\text{ref}}^2}\right) = 83.2 + \frac{19.3}{(\frac{T_r}{T_\infty})^{0.62}} + 10\log\left(\frac{V_j}{a_\infty}\right)^n \quad (9)$$

where

$$n = 6.4 + \frac{1.2}{(\frac{T_r}{T_\infty})^{1.4}}. \quad (10)$$

According to (10) the velocity exponent is equal to 7.6 for cold jets. This is very close to the well-known subsonic jet value of 8. However, the jet temperature exerts a fairly strong effect. At a jet temperature ratio of 2, the value of n drops to 6.85. Because the second term on the right side of equation (9) is not as sensitive to jet temperature, overall the noise level is not as greatly reduced by increase in jet temperature (at a fixed velocity). For reference purpose, we note that there is an approximately 6.7 dB noise reduction between a jet at temperature ratio of 2 and that of a cold jet at a fixed jet velocity.

In analyzing the dependence of the peak frequency, f_L, of the large turbulence structures/instability waves noise on jet operating con-

ditions at the maximum amplitude direction, we noticed a somewhat curious phenomenon. Figure 10 shows the variation of the measured peak Strouhal number based on ambient sound speed, $f_L \frac{D_j}{a_\infty}$, with $\frac{V_j}{a_\infty}$ at $\chi = 160$ deg. As the jet velocity decreases toward $\frac{V_j}{a_\infty} = 1$ this peak Strouhal number, instead of increasing, appears to level off and reach an asymptote of 0.19. The asymptote value is not sensitive to the jet temperature. Currently we do not know why the peak Strouhal number in the transonic range should be more or less constant at 0.19. We wish to point this out for it seems to be related to a similar phenomenon observed by Ahuja[18] in subsonic jets.

A point that is of interest to us is the relative dominance of the two noise components with respect to the direction of radiation and jet operating parameters. To assign relative dominance without excessive data analysis, we simply compare the peak amplitudes A and B. Experimentally, the data available to us is not fine enough to establish a sharp demarcation line in the jet operating parameter space to delineate the region of dominance of each noise component. The best we can do is to give a somewhat broad transition region. It must be reminded that, near the transition boundary, both noise components are of equal importance. A firm statement of dominance can only be made away from the transition boundary. Figure 11 is a plot of the transition boundary at different jet to ambient temperature ratio in the $\frac{V_j}{a_\infty}$ versus χ plane. Large turbulence structures/instability waves noise is dominant in the lower right-hand corner of the figure. Fine-scale turbulence noise is dominant in the upper left-hand corner. With increase in jet temperature, the transition boundary moves up and to the left. What this means is that at a fixed jet velocity, large turbulence structures/instability waves noise is dominant over a larger angular sector for hot jets. On the other hand, at a fixed jet temperature ratio (e.g. cold jets) increase in jet velocity (or Mach number) tends to increase the angular sector of dominance of the fine-scale turbulence noise.

4. Imperfectly Expanded Jets

Supersonic jets from convergent-divergent nozzles are often operated at off-design conditions. Under this circumstance, a shock cell structure develops inside the jet plume. Of importance is whether the presence of the shock cell structure would affect the turbulent mixing noise of the jet when compared with an equivalent fully-expanded jet. Kim, Kresja and Khavaran[19] recently compared the noise of a perfectly expanded jet from a C-D nozzle and that of an underexpanded jet from a convergent nozzle at a pressure ratio of 3.3. They provided evidence that the turbulent mixing noise spectra at several selected angles were nearly identical. Thus the presence of a shock cell structure does not materially affect the turbulent mixing noise.

In this investigation, we carried out a thorough comparison between the noise spectra of underexpanded, perfectly expanded and overexpanded jets at Mach number 1.37, 1.5, 1.8 and 2.0 and jet temperature ratio of 1.0 to 2.26. The purpose is to find out what are the effects of the presence of a shock cell structure in the jet flow on each of the two components of turbulent mixing noise. It is well-known that in the presence of a quasi-periodic shock cell structure, supersonic jets radiate an additional noise component with discrete frequency called screech tones[3]. Screech tones are generated by a feedback loop. When the tone intensity is low, it has been found experimentally that the feedback loop does not significantly affect the jet flow such as the jet spreading rate and the jet core length. As a result, both the large turbulence structures/instability waves noise and the fine-scale turbulence noise are nearly unaffected. Figure 12 compares the fine-scale turbulence noise from a perfectly expanded and an underexpanded jet at $M_j = 1.49$ and $\frac{T_r}{T_\infty} = 2.25$ at $\chi = 90$ deg. If the broadband shock associated noise of the underexpanded jet is ignored, there is good agreement between the two measured noise spectra. Both spectra, in turn, fit the similarity spectrum well. Figure 13 compares the noise spectra of the same two jets at $\chi = 138$ deg. In this direction, the noise is dominated by the large turbulence structures/instability waves noise. As can be seen there is good agreement between the measured data and the similarity noise spectrum. Figure 14 provides examples of typical comparison between the noise spectra of fine-scale turbulence from overexpanded and underexpanded jets at $\chi = 90$ deg. The lower figure is for $M_j = 1.37$ at a jet temperature ratio of around 1.8. The top figure is for $M_j = 1.8$ at $\frac{T_r}{T_\infty} = 2.2$. Evidently, there is good agreement between the fine-scale turbulence noise spectra of these jets. Both spectra appear to fit the similarity spectrum well. Figure 15 shows similar comparisons for the large turbulence structures/instability waves noise of the same jets at $\chi = 139.4$ deg. Again there are good agreements between the measured noise spectrum and the empirical spectrum of equation (5). Figure 16 shows typical comparisons of the noise spectra of underexpanded and overexpanded jets at intermedi-

ate angle of radiation ($\chi = 112.6$ deg) where both noise components contribute to the total turbulent mixing noise. Overall, the agreement between the two measured spectra and the combined empirical similarity spectrum is good.

Under certain jet operating conditions, the screech tones of an imperfectly expanded jet can be very intense. When this happens, the jet flow is drastically changed and the turbulence level is greatly increased. One would, therefore, expect an enhancement of the radiated noise. Figure 17 provides experimental evidence of broadband amplification of fine-scale turbulence noise by strong screech. Curve (a) is the noise spectrum of a perfectly expanded jet at $M_j = 1.49$, $\frac{T_r}{T_\infty} = 1.0$ and $\chi = 112.6$ deg. The spectrum fits the similarity spectrum shape fairly well. Curve (b) shows the spectrum of a nearly identical underexpanded jet undergoing strong screeching. The spectrum is similar in shape to that of the perfectly expanded jet except that it is about 3 dB higher across all frequencies of the spectrum. This phenomenon does not seem to have been observed before. It is, however, very similar to the so-called "broadband noise amplification" phenomenon observed in subsonic jets[20-22]. In the subsonic jet case, the jet noise spectrum is enhanced by 3–4 dB across nearly the entire frequency range of measurement when the jet is excited internally or externally by a pure tone. A nonlinear integral model which has proven to be able to provide fairly accurate prediction of the enhanced pressure fluctuation in the jet flow is available[23]. However, the precise process which helps to maintain the shape of the radiated noise spectrum of the excited jet remains unknown.

The effect of strong screech on the large turbulence structures/instability waves noise of a supersonic jet is illustrated in figure 18. Curves (a) and (b) are measurements from the same jets as figure 17 but at an inlet angle of 139.4 deg. In this direction the large turbulence structures/instability waves noise is dominant. Again, there is broadband amplification of the radiated noise by about 3 dB. Presently, we have no explanation of the physical processes involved.

It is known[3] that strong screech tones are generated in the region between the third and fourth shock cells of the jet by intense interaction between the instability waves of the jet flow and the shock cell structure. This process naturally leads to enhanced production of fine-scale turbulence and hence noise. We believe that jet noise and turbulence are generated simultaneously. Noise from decaying turbulence is relatively unimportant. From this point of view, the dominant source of fine-scale turbulence noise must be located in the core region of the jet centered around the fourth shock cell.

5. Turbulent Mixing Noise from Subsonic Jets

Our data correlation effort has indicated to us that M_j, the fully expanded jet Mach number, is not a useful parameter for characterizing turbulent mixing noise. But if M_j is unimportant, then our finding that turbulent mixing noise consists of two distinct components should be true regardless of M_j. In other words, it must be valid for supersonic jets ($M_j > 1$) as well as subsonic jets ($M_j < 1$). However, one might argue that the difference between subsonic and supersonic jets is not so much in M_j being less than or greater than 1, but in the effect of compressibility. There is a general belief that compressibility effects are more important in supersonic jets than subsonic jets and that this might have significant impact on the noise generation processes. Recently, experimental measurements by Papamoschou and Roshko[24], Bogdanoff[25] and others demonstrated conclusively that compressibility effects are not related to M_j but to the convective Mach number M_c. Compressibility effects become important in turbulent mixing only when M_c is near or larger than 1. For static jets, up to moderate supersonic Mach number, M_c is small. Therefore, there is no reason to believe there should be a drastic change in the turbulent mixing noise generation mechanism between subsonic and supersonic jets.

If indeed, turbulent mixing noise of subsonic jets is made up of two components, one of which is noise from the large turbulence structures/instability waves, one would like to know how Mach wave radiation can be accomplished in such low speed jets. In the original discussion on Mach wave radiation, Tam and Burton[4] emphasized the importance of the spatial growth and decay of the instability wave amplitude on noise radiation. They noted that a subsonic wave of constant amplitude would not generate sound in a compressible medium. Such a wave has a discrete wavenumber spectrum. However, for a fixed-frequency instability wave whose amplitude undergoes growth and decay spatially, its wavenumber spectrum is no longer discrete. Instead, it is broadband. Some of these broadband wave components, especially those with small wavenumbers, would actually be moving with supersonic phase velocities. These supersonic phase

velocity disturbances, by the wavy-wall analogy, will immediately lead to Mach wave radiation. As the jet speed becomes more and more subsonic, the fraction of the wavenumber spectrum which has supersonic phase velocity becomes smaller and clusters around the sonic wavenumber. The Mach waves would, therefore, be radiated only in directions closed to the jet axis. The broadening of the wavenumber spectrum by the growth and decay of the instability wave amplitude is most effective if the growth is rapid followed by an equally rapid decay. It is known from jet instability wave calculations that the growth and decay rates of instability waves in subsonic jets are much higher than those of supersonic jets. Because of this, it is, therefore, possible for large turbulence structures/instability waves to produce Mach wave radiation even when the jet Mach number is low subsonic.

It is well documented experimentally[21] and theoretically[27] since the 1960's that sound refraction by the mean flow of a subsonic jet creates a cone of silence for the fine-scale turbulence noise around the direction of the jet flow. On the other hand, as pointed out above, this is the principle direction of Mach wave radiation by the large turbulence structures/instability waves. Thus the noise spectrum and characteristics inside the cone of silence of the fine-scale turbulence noise of a subsonic jet should be those associated with Mach wave radiation alone. They would, therefore, be distinctly different from noise radiated at angles outside the cone of silence. The experimental measurements of Lush[28] and Ahuja[18] prove that this is, indeed, the case. Inside the cone of silence, their measured noise intensity is not only not small; it is the highest. Moreover, the spectrum shape is distinctly different from those in directions at larger exhaust angles.

To provide concrete experimental evidence that turbulence mixing noise from subsonic jets, just as their supersonic counterparts, consists of two distinct components, we converted all the data of Ahuja which was measured in one-third octave band into narrow band data scaled to a distance of $100D_j$. Admittedly, there is a loss of accuracy in this process. But the converted data allows us to make quantitative comparisons with the similarity noise spectra and with our supersonic jet noise data.

Figure 19 shows the narrow band noise spectrum (in dB per 1 Hz band) of a Mach 0.98 jet measured by Ahuja at $\frac{T_r}{T_\infty} = 1.0$ and $\chi = 160$ deg (inside the cone of silence). The smooth curve in this figure is the similarity spectrum $10 \log F$ of figure 2 or equation (5) with amplitude A and peak frequency f_L adjusted so that the peaks of the two spectra coincide. It is evident that the curve is an excellent fit to the data providing irrefutable evidence that this is, in fact, the noise from the large turbulence structures/instability waves of the subsonic jet. Figure 10 shows the corresponding measured noise spectrum at $\chi = 90$ deg. In this direction, the noise is from the fine-scale turbulence. Here the smooth curve is the similarity noise spectrum of $10 \log G$ (equation (6)) of the fine-scale turbulence. The agreement between the data and the similarity noise spectrum is very good giving strong support to our contention that the second component of turbulent mixing noise from subsonic jets is, as in the case of supersonic jets, fine-scale turbulence noise.

To provide further evidence that the turbulent mixing noise generation mechanisms are the same regardless of jet Mach number, i.e., whether it is subsonic or supersonic, we plot the measured value of the peak noise intensity, $10 \log(\frac{A}{p^2_{\text{ref}}})$ in dB per 1 Hz band at $\chi = 160$ deg of the data of Ahuja in figure 8. They are the data point with $\frac{V_j}{a_\infty} < 1$. It is clear that the subsonic jet noise data falls on the same straightline as the supersonic jet noise data. This proves that there is no change in the Mach wave noise generation mechanism even when the jet is subsonic. We have also plotted the measured values of $10 \log(\frac{B}{p^2_{\text{ref}}})$ in dB per 1 Hz band at $\chi = 90$ deg from the data of Ahuja in figure 9. They form the natural straightline extension of our supersonic jet noise data. Thus empirical noise intensity formulas (7) and (9), developed for supersonic jets, are also valid for subsonic jets.

It was noticed by Ahuja[18] that for noise radiated in the direction $\chi = 160$ deg the frequency at the peak of the spectrum, f_L, remained the same independent of the jet Mach number. He found that $f_L \frac{D}{a_\infty} = 0.2$. This is the black line shown in figure 10. It matches well the value of the asymptote of our supersonic jet noise data. The slight difference in the two values is due mainly to that Ahuja picked his value of f_L from one-third octave band spectra and hence would be higher than our narrow band value. The fact that there is such good agreement between the subsonic and supersonic jet data leaves very little room for doubt that large turbulence structures/instability waves noise is, indeed, a component of subsonic jet noise.

Since the beginning of jet noise research in the early fifties, the Acoustic Analogy Theory [29–31]

has maintained that subsonic jet noise is generated by quadrupoles. Physically, it is not clear what quadrupoles are in turbulent flows. They are quantities foreign to the main stream turbulence research community. With quadrupoles as the only noise source, the theory implies that there is one component of turbulent mixing noise. The evidence we have presented are clearly at odds with this classical theory. We believe that the Acoustic Analogy Theory, having failed to predict many of the salient jet noise characteristics, is not a good starting point for jet noise prediction. A new theory based on two distinct noise components and improved turbulence physics is badly needed.

6. Nonaxisymmetric Jets

As a part of the present investigation, a pilot study of the noise from nonaxisymmetric supersonic jets was carried out. The sole purpose was to make a preliminary assessment if there are basic differences in the noise generation mechanisms between these jets and axisymmetric jets. The pilot study was confined to rectangular and elliptic jets alone. Data for rectangular jets was measured using a 2-D convergent-divergent nozzle of aspect ratio 7.6, design Mach number 2.0 and exit dimensions 1.355 cm × 10.243 cm. The elliptic nozzle had an aspect ratio of 3, design Mach number 1.98 and exit dimensions 6.096 cm (major axis) × 1.016 cm (minor axis).

Figure 21 shows comparisons between measured noise spectra and the similarity spectrum $10\log F$ of figure 2 or equation (5) for both the rectangular and elliptic jets at $\chi = 130$ deg. The sample data include jets operated at design and off-design conditions. The jet to ambient temperature ratio varies from 1.8 to 2.26. ϕ is the azimuthal angle between the measurement plane and the reference plane which is the symmetric plane passing through the minor axis of the nozzle. All the spectra in the figure fit the similarity spectrum well. This indicates that large turbulence structures/instability waves noise is also a major noise component of these two types of jets.

Figure 22 shows comparisons between the measured noise spectra and the similarity spectrum $10\log G$ of figure 2 or equation (6). The data in this figure were measured at $\chi = 89$, 95 and 108 deg in the major or the minor axis plane. At these angular directions, the fine-scale turbulence noise is dominant. As can be readily seen there is good agreement between all the measured spectra and the similarity spectrum. This assures us that the fine-scale turbulence noise generation mechanism of these jets is the same as axisymmetric jets.

We would like to emphasize here that our pilot study is only preliminary in nature. It is definitely not comprehensive. For nonaxisymmetric jets, suggestions have been made recently of the possible existence of longitudinal vortices in the jet plume. It was speculated that these longitudinal vortices could exert significant modifications to the jet flow and radiated noise. So far, we have, however, not found any evidence that the noise generation mechanisms of these jets are not the same as those of the axisymmetric jets. But in the absence of a comprehensive study, we cannot rule out such possibilities at this time. Also, there are non-simple nonaxisymmetric jets such as those from lobed nozzles. Their noise characteristics and noise generation mechanisms could conceivably be very different from what we have found in this investigation.

7. Summary and Discussion

In this paper, we have presented extensive experimental evidence showing that turbulent mixing noise from both supersonic and subsonic jets is composed of two components. One component is the noise of the large turbulence structures/instability waves of the jet flow. The other is the noise of the fine-scale turbulence. The similarity spectra for both noise components are found empirically. These spectra, however, have rather universal applicability. They fit all our axisymmetric supersonic jet data and the subsonic jet data of Ahuja regardless of the jet Mach number, the jet temperature ratio, the direction of radiation and whether the jet is perfectly or imperfectly expanded. Furthermore, they also fit the rectangular and elliptic supersonic jet noise data that we have processed.

For supersonic jets undergoing strong screeching, a broadband noise amplification phenomenon is identified. For such jets, there is an increase in the noise intensity of both turbulent mixing noise components across the entire jet noise spectrum. The underlying physical processes responsible for the phenomenon, however, remain unknown.

Over the last forty years, the Acoustic Analogy Theory advocates that subsonic jet noise is generated by moving quadrupoles. Our present finding does not support this theory. Experimental evidence clearly shows, just like supersonic jets, turbulent mixing noise of subsonic jets consists of two distinct components; the fine-scale turbulence noise and the large turbulence structures/instability waves noise.

Further, jet Mach number is not an effective correlation parameter of jet turbulent mixing noise. As far as this jet noise component is concerned, $M_j = 1$ has no real significance.

The noise of a jet is generated by the turbulence of the jet flow. The fact that there are two distinct noise components implies that there must be two distinct types of turbulent motion in the jet flow. Since the frequencies of the two noise components overlap, the two types of turbulent motion must have overlapping frequencies. With the frequencies the same, the only possibility is that the spatial scales of the two types of turbulent motion of the jet flow are different. That is, the turbulence of the jet consists of very large scale turbulent motion and very fine-scale motion with little energy for the scales in between. This, in turn, suggests that there is no continuous cascading of the large-scale turbulence structures into smaller and smaller scale turbulence until the fine-scale turbulence is reached. The continuous cascading scenario is ruled out for otherwise there would be a considerable amount of turbulence belonging to the intermediate scales. It appears, therefore, the large turbulence structures extract energy from the mean flow as they grow and give up their energy back to the mean flow as they decay. This is exactly the behavior of instability waves. Thus large turbulence structures and instability waves are effectively one and the same entity in turbulent jet flows.

Table 1. Dimensions and Characteristics of the Jet Nozzles Used in the NASALangley Experiments

M_d	D (cm)	Nozzle type	range of M_j	range of $\frac{T_j}{T_\infty}$
1.0	3.952	C†	1.37 to 1.8	1.0 to 2.24
1.5	4.267	CD*	1.37 to 1.8	1.0 to 2.35
2.0	4.989	CD	1.5 to 2.24	1.0 to 2.26
2.0	9.144	CD	2.0	1.12 to 4.9

† =convergent, * =convergent-divergent

Acknowledgments

The work of CKWT was supported by NASA Langley Research Center Grant NAG 1-1776. The authors wish to thank K.K. Ahuja for providing them with his subsonic jet noise data in tabulated form.

References

1. Tam, C.K.W. and Chen, P., "Turbulent Mixing Noise from Supersonic Jets," *AIAA J.*, **32**, Sept. 1994, pp. 1774–1780.

2. Seiner, J.M. and Kresja, E.A., "Supersonic Jet Noise and the High Speed Civil Transport," AIAA Paper 89–2358, July 1989.

3. Tam, C.K.W., "Supersonic Jet Noise," *Annual Review of Fluid Mechanics*, **27**, 1995, pp. 17–43.

4. Tam, C.K.W. and Burton, D.E., "Sound Generated by Instability Waves of Supersonic Flows. Part I: Two Dimensional Mixing Layers. Part 2: Axisymmetric Jets." *J. Fluid Mech.*, **138**, Jan. 1984, pp. 249–295.

5. Seiner, J.M., Ponton, M.K., Jansen, B.J. and Lagen, N.T., "The Effects of Temperature on Supersonic Jet Noise Emission," AIAA Paper 92-02-046, May 1992, DGLR/AIAA 14th Aeroacoustics Conference, Aachen, Germany.

6. Seiner, J.M., Bhat, T.R.S. and Ponton, M.K., "Mach Wave Emission from a High-Temperature Supersonic Jet," *AIAA J.*, **32**, Dec. 1994, pp. 2345–2350.

7. Yu, J.C., "Investigation of the Noise Field of Supersonic Axisymmetric Jet Flow," Ph.D. Thesis, Dept. of Mech. Eng., Syracuse University, Apr. 1971.

8. Yu, J.C. and Disanjh, D.S., "Noise Field of Supersonic Mach 1.5 Cold Model Jet," *J. Acous. Soc. Amer.*, **51**, Sept. 1992, pp. 1400–1410.

9. Norum, T.D. and Seiner, J.M., "Measurements of Static Pressure and Far Field Acoustics of Shock-Containing Supersonic Jets," NASA TM 84521, Sept. 1982.

10. Tanna, H.K., "An Experimental Study of Jet Noise, Part I: Turbulent Mixing Noise; Part II: Shock Associated Noise," *J. Sound and Vibration*, **50**, 1977, pp. 405–444.

11. Eggers, J.M., "Velocity Profiles and Eddy Viscosity Distributions Downstream of a Mach 2.22 Nozzle Exhausting to Quiescent Air," NASA TN-3601, 1966.

12. Lau, J.C., Morris, P.J. and Fisher, M.J., "Measurements in Subsonic and Supersonic Free Jets Using a Laser Velocimeter," *J. Fluid Mech.*, **93**, 1979, pp. 1–27.

13. Lau, J.C., "Effects of Exit Mach Number and

Temperature on Mean-Flow and Turbulence Characteristics in Round Jets," *J. Fluid Mech.*, **105**, 193–218.

14. Seiner, J.M., McLaughlin, D.K. and Liu, C.H., "Supersonic Jet Noise Generated by Large Scale Instabilities," NASA TP-2072, Sept. 1982.
15. Tam, C.K.W., "Broadband Shock Associated Noise of Moderately Imperfectly Expanded Supersonic Jets," *J. Sound and Vibration*, **140**, 1988, pp. 55-71.
16. Tam. C.K.W., "Broadband Shock Associated Noise from Supersonic Jets in Flight," *J. Sound and Vibration*, **151**, 1991, pp. 131–147.
17. Tam, C.K.W., "Broadband Shock Associated Noise from Supersonic Jets Measured by a Ground Observer," *AIAA J.*, **30**, Oct. 1992, pp. 2395–2401.
18. Ahuja, K.K., "Correlation and Prediction of Jet Noise," *J. Sound and Vibration*, **29**, No. 2, 1973, pp. 155–168.
19. Kim, C.M., Kresja, E.A. and Kavaran, A., "Significance of Shock Structure on Supersonic Mixing Noise of Axisymmetric Nozzles," *AIAA J.*, **32**, Sept. 1994, pp. 1920–1923.
20. Bechert, D. and Pfizenmaier, E., "On the Amplification of Broadband Jet Noise by Pure Tone Excitation," *J. Sound and Vibration*, **43**, 1975, pp. 581–587.
21. Moore, C.J., "The Role of Shear-Layer Instability Waves in Jet Exhaust Noise," *J. Fluid Mech.*, **80**, 1977, pp. 321–367.
22. Ahuja, K.K. and Blakney, D.F., "Tone Excited Jets, Part IV: Acoustic Measurements," *J. Sound and Vibration*, **102**, No. 1, 1985, pp. 93–118.
23. Tam. C.K.W. and Morris, P.J., "Tone excited Jets, Part V: A Theoretical Model and Comparison with Experiment," *J. Sound and Vibration*, **102**, No. 1, 1985, pp. 119–151.
24. Papamoschou, D. and Roshko, A., "The Compressible Turbulent Shear Layers: An Experimental Study," *J. Fluid Mech.*, **197**, 1988, pp. 453–477.
25. Bogdanoff, D.W., "Compressible Effects in Turbulent Shear Layers," *AIAA J.*, **21**, 1983, pp. 926–927.
26. Atvars, J., Schubert, L.H., and Ribner, H.S., "Refraction of Sound from a Point Source Placed in an Air Jet," *J. Acous. Soc. Amer.*, **37**, 1965, pp. 168–170.
27. Schubert, L.H., "Numerical Study of Sound Refraction by a Jet Flow. I: Ray Acoustics; II: Wave Acoustics," *J. Acous. Soc. Amer.*, **51**, 1972, pp. 439–463.
28. Lush, P.A., "Measurements of Subsonic Jet Noise and Comparison with Theory," *J. Fluid Mech.*, **46**, part 3, 1971, pp. 477–500.
29. Lighthill, M.J., "On Sound Generated Aerodynamically: I. General Theory," *Proc. Roy. Soc. London, Ser. A*, **211**, Mar. 1952, pp. 564–587.
30. Lighthill, M.J., "On Sound Generated Aerodynamically: II. Turbulence as a Source of Sound," *Proc. Roy. Soc. London, Ser. A*, **222**, Feb. 1954, pp. 1–32.
31. Lilley, G.M., "Jet Noise Classical Theory and Experiments," Chapter 4 of *Aeroacoustics of Flight Vehicles: Theory and Practice*, ed. H.H. Hubbard, NASA RP-1258, Aug. 1991, pp. 211–289.

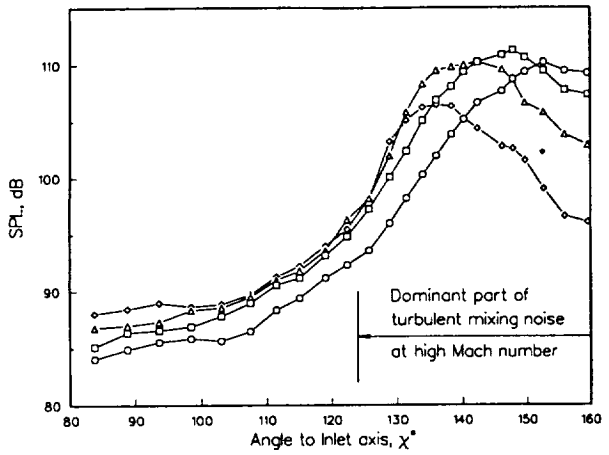

Figure 1. Measured[5] noise directivities at selected Strouhal numbers of a Mach 2 jet at a total temperature of 500 K ($St = fD/U_j$) O St=0.067; □ St=0.12; Δ St=0.20; ◇ St=0.40.

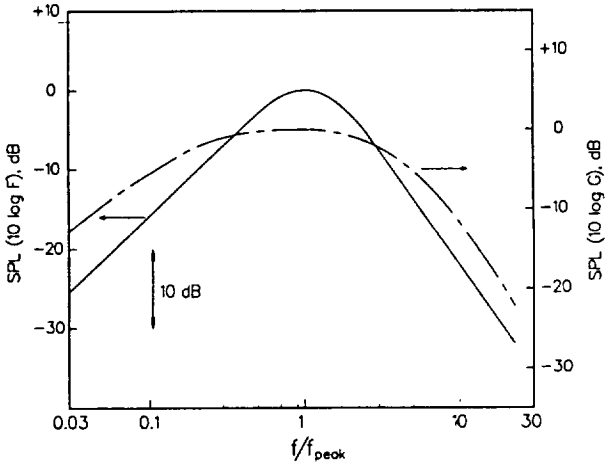

Figure 2. Similarity spectra for the two components of turbulent mixing noise. ——— large turbulence structures/ instability waves noise; — - — - fine scale turbulence noise.

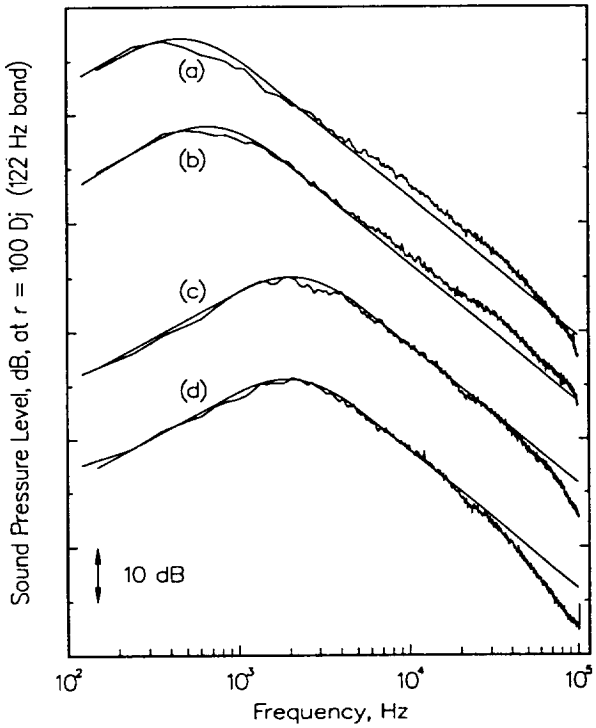

Figure 3. Comparison of the similarity spectrum of large turbulence structures/instability waves noise and measurements.
(a) $M_j = 2.0$, $T_r/T_\infty = 4.89$, $\chi = 160.1°$, $SPL_{max} = 124.7$ dB,
(b) $M_j = 2.0$, $T_r/T_\infty = 1.12$, $\chi = 160.1°$, $SPL_{max} = 121.6$ dB,
(c) $M_j = 1.96$, $T_r/T_\infty = 1.78$, $\chi = 138.6°$, $SPL_{max} = 121.0$ dB,
(d) $M_j = 1.49$, $T_r/T_\infty = 1.11$, $\chi = 138.6°$, $SPL_{max} = 106.5$ dB.

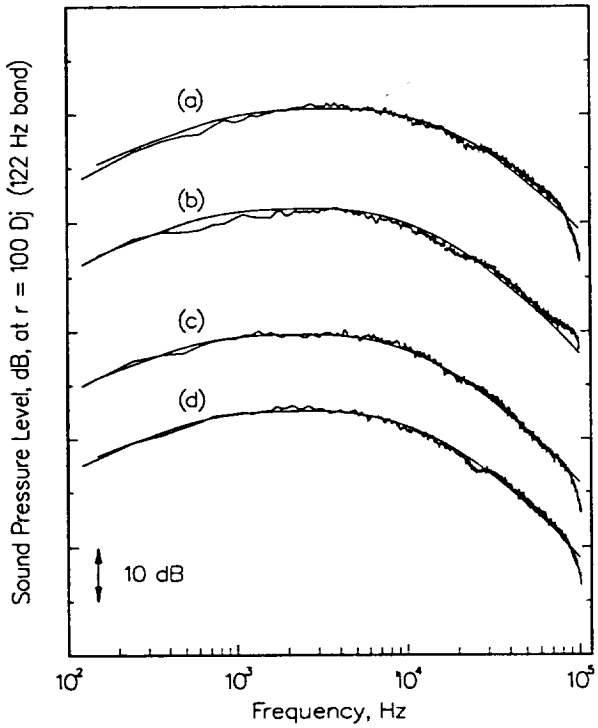

Figure 4. Comparison of the similarity spectrum of fine scale turbulence and measurements.
(a) $M_j = 1.49$, $T_r/T_\infty = 2.35$, $\chi = 92.9°$, $SPL_{max} = 96$ dB,
(b) $M_j = 2.0$, $T_r/T_\infty = 4.89$, $\chi = 83.8°$, $SPL_{max} = 107$ dB,
(c) $M_j = 1.96$, $T_r/T_\infty = 0.99$, $\chi = 83.3°$, $SPL_{max} = 95$ dB,
(d) $M_j = 1.96$, $T_r/T_\infty = 0.98$, $\chi = 120.2°$, $SPL_{max} = 100$ dB.

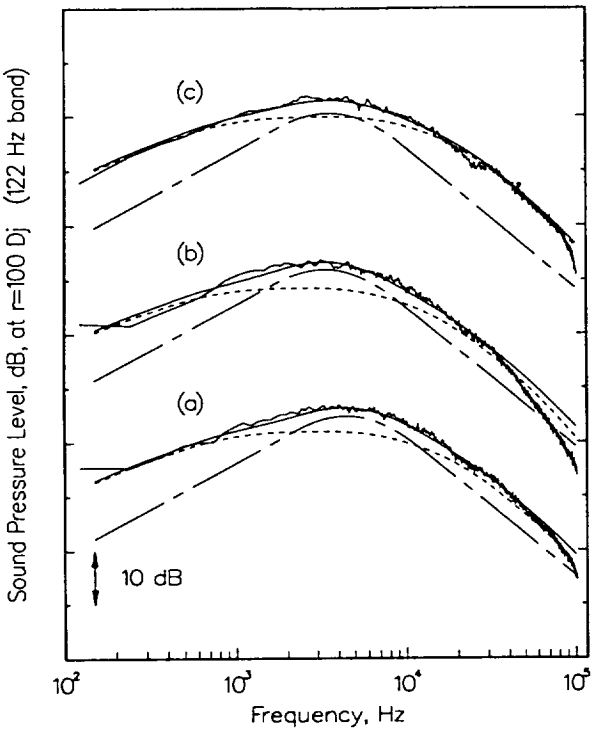

Figure 5. Comparison of the sum of the similarity spectra of both large and fine scale turbulence noise and measurements at intermediate direction of radiation. — - — large turbulence structures noise; - - - - - fine scale turbulence noise; ——— total.
(a) $M_j = 1.49$, $T_r/T_\infty = 2.25$, $\chi = 112.6°$, $SPL_{max} = 101.5$ dB,
(b) $M_j = 1.49$, $T_r/T_\infty = 1.33$, $\chi = 126.9°$, $SPL_{max} = 100.5$ dB,
(c) $M_j = 1.96$, $T_r/T_\infty = 1.79$, $\chi = 120.2°$, $SPL_{max} = 107.0$ dB,

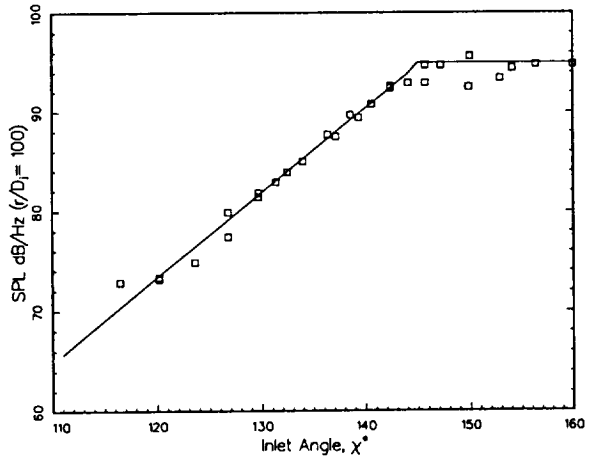

Figure 6. Variation of the peak amplitude of the noise spectrum of large turbulence structures/instability waves with direction of radiation. $M_j = 1.8$, $T_r/T_\infty = 1.0$

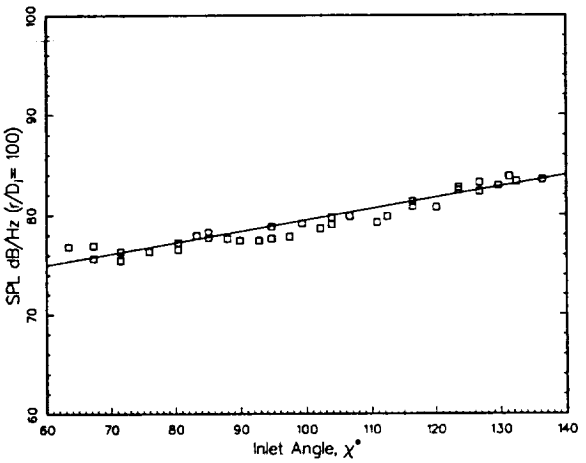

Figure 7. Variation of the peak amplitude of the noise spectrum of fine scale turbulence with direction of radiation. $M_j = 2.24$, $T_r/T_\infty = 1.0$

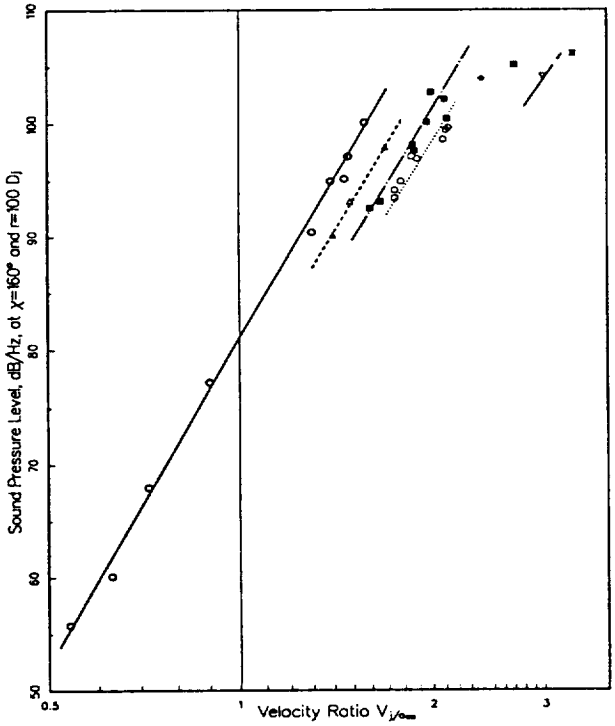

Figure 8. Variation of the peak amplitude of the noise spectrum of large turbulence structures/instability waves at $\chi = 160°$ with jet velocity and temperature ratios.

T_r/T_∞	1.0	1.4	1.8	2.2
measurements	○	△	■	○
Equation (7)	———	- - - - -	— · —	·····
T_r/T_∞	2.7	3.3	4.1	4.9
measurements	◆	⊠	▽	⧈
Equation (7)			— - —	

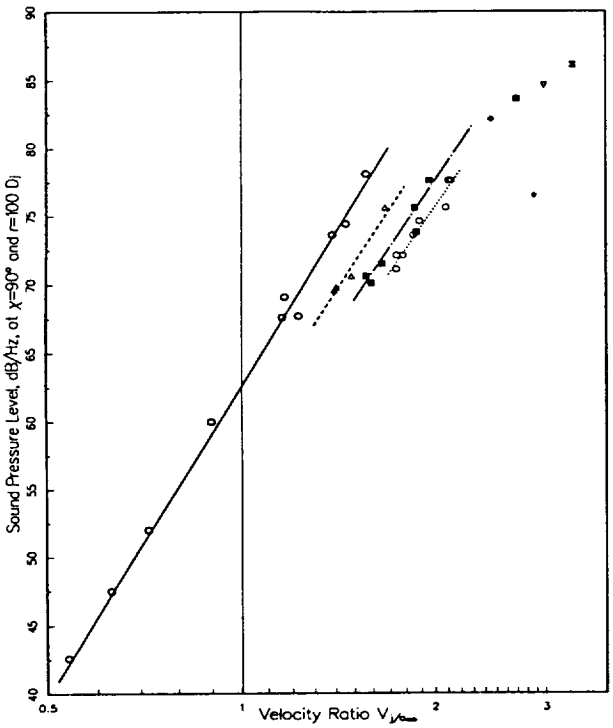

Figure 9. Variation of the peak amplitude of the noise spectrum of fine scale turbulence at $\chi = 90°$ with jet velocity and temperature ratios.

T_r/T_∞	1.0	1.4	1.8	2.2
measurements	○	△	■	○
Equation (9)	———	- - - - -	— · —	·····
T_r/T_∞	2.7	3.3	4.1	4.9
measurements	◆	⊠	▽	⧗
Equation (9)			— - —	

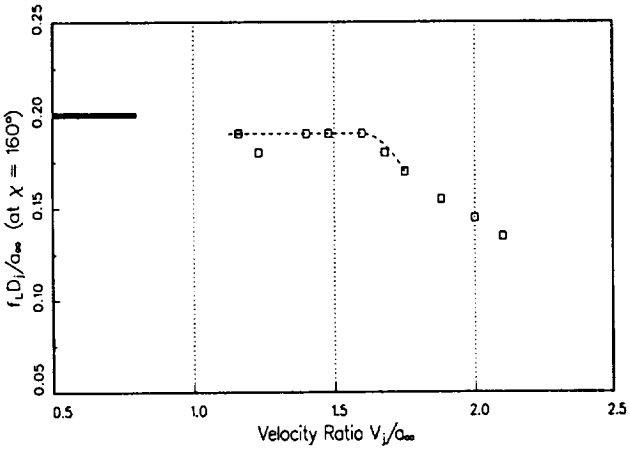

Figure 10. Variation of the Strouhal number at the spectrum peak of the large turbulence structure/instability waves noise at $\chi = 160°$ with jet velocity ratio.

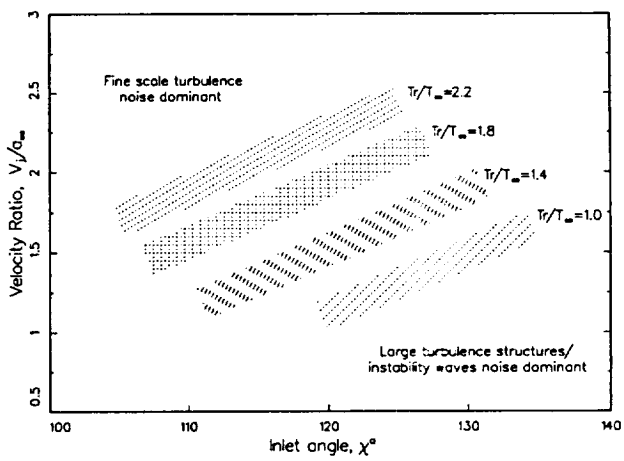

Figure 11. Diagram showing the region of dominance of the two turbulent mixing noise components in the parameter space of inlet angle, velocity and temperature ratio. Shaded regions indicate nearly equal peak SPL.

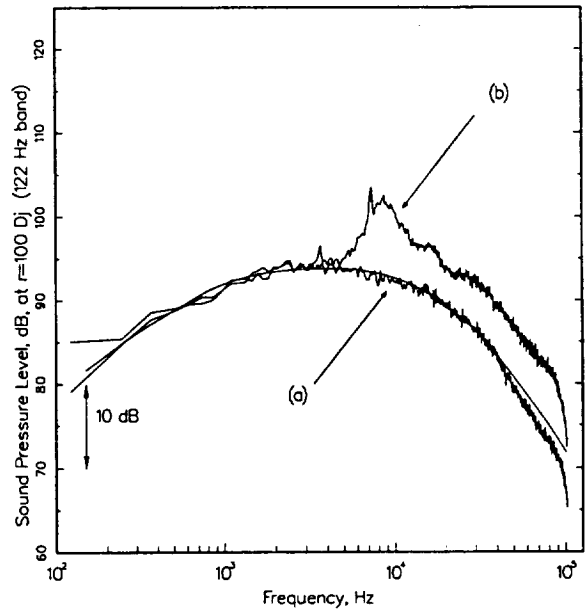

Figure 12. Comparison of the fine scale turbulence noise spectrum from a perfectly expanded and an underexpanded jet at $T_r/T_\infty = 2.25$. (a) $M_j = M_d = 1.49$, $\chi = 90°$, (b) $M_j = 1.49$, $M_d = 1.0$, $\chi = 90°$

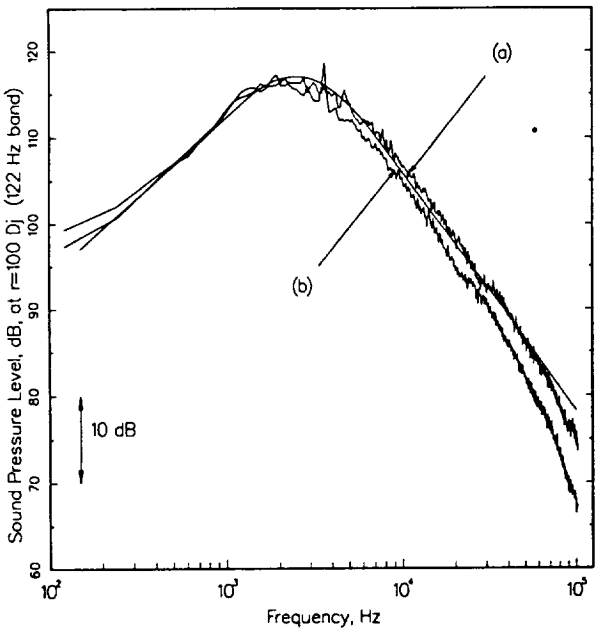

Figure 13. Comparison of the large turbulence structure/instability waves noise spectrum from a perfectly expanded and an underexpanded jet at $T_r/T_\infty = 2.25$. (a) $M_j = M_d = 1.49$, $\chi = 137.3°$,
(b) $M_j = 1.49$, $M_d = 1.0$, $\chi = 138.6°$.

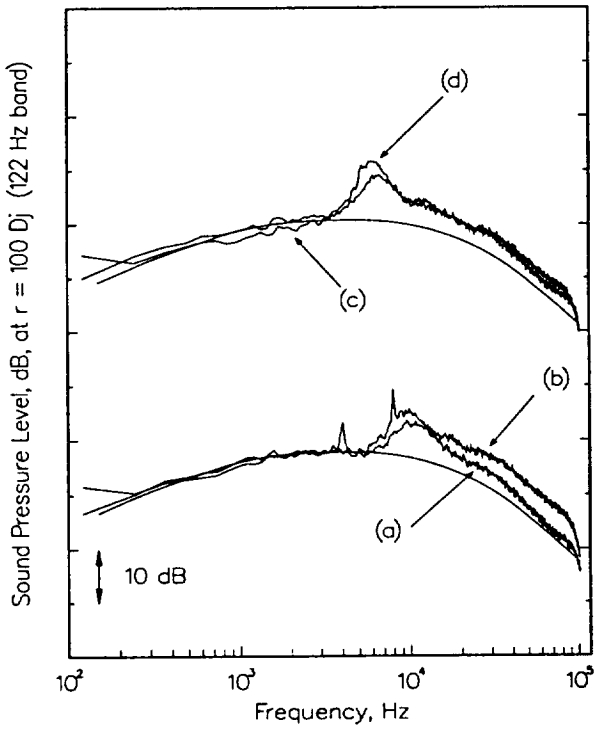

Figure 14. Comparison of the noise spectra of fine scale turbulence noise from overexpanded and underexpanded jets at $\chi = 90.0°$.
(a) $M_j = 1.37$, $M_d = 1.5$, $T_r/T_\infty = 1.81$, $SPL_{max} = 98$ dB,
(b) $M_j = 1.37$, $M_d = 1.0$, $T_r/T_\infty = 1.87$, $SPL_{max} = 104$ dB,
(c) $M_j = 1.8$, $M_d = 2.0$, $T_r/T_\infty = 2.26$, $SPL_{max} = 106$ dB,
(d) $M_j = 1.8$, $M_d = 1.5$, $T_r/T_\infty = 2.22$, $SPL_{max} = 111$ dB.

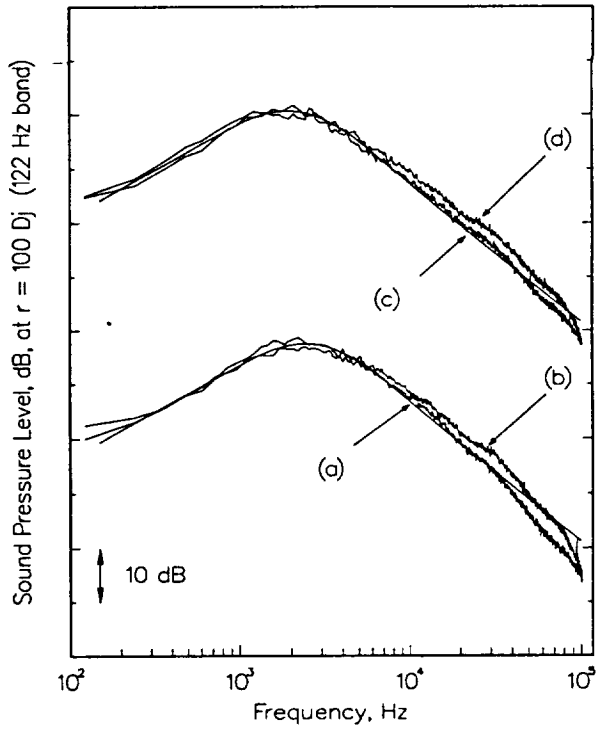

Figure 15. Comparison of the noise spectra of large turbulence structures/instability waves from overexpanded and underexpanded jets at $\chi = 139.4°$.
(a) $M_j = 1.37$, $M_d = 1.0$, $T_r/T_\infty = 1.81$, $SPL_{max} = 114$ dB,
(b) $M_j = 1.37$, $M_d = 1.5$, $T_r/T_\infty = 1.87$, $SPL_{max} = 112$ dB,
(c) $M_j = 1.8$, $M_d = 2.0$, $T_r/T_\infty = 2.26$, $SPL_{max} = 120$ dB,
(d) $M_j = 1.8$, $M_d = 1.5$, $T_r/T_\infty = 2.22$, $SPL_{max} = 121$ dB.

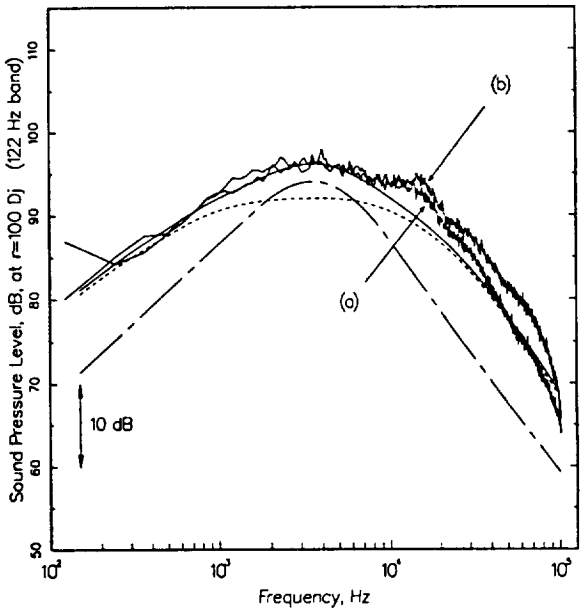

Figure 16. Comparison of the combined spectrum of large and fine scale turbulence noise from an overexpanded and an underexpanded jet at intermediate angle of radiation. — - — large turbulence structures noise; - - - - - fine scale turbulence noise; ——— total $T_r/T_\infty = 1.8$, $\chi = 112.6°$, (a) $M_j = 1.37$, $M_d = 1.5$, (b) $M_j = 1.37$, $M_d = 1.0$.

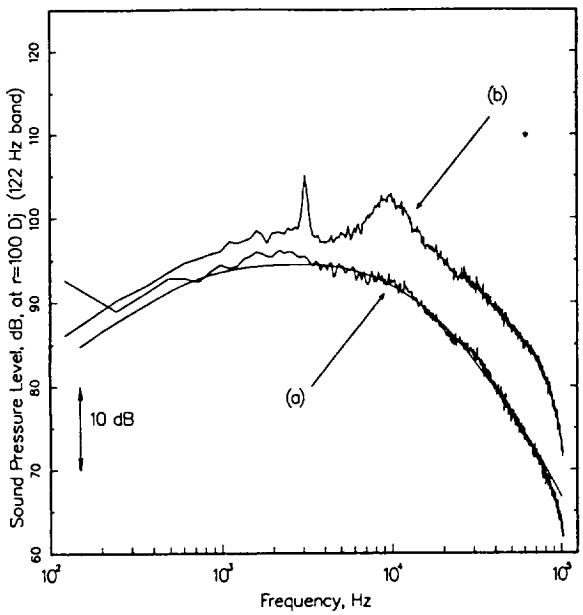

Figure 17. Experimental evidence of broadband amplification of fine scale turbulence noise in the presence of strong screech. $T_r/T_\infty = 1.0$, $\chi = 112.6°$, (a) $M_j = M_d = 1.49$, (b) $M_j = 1.49$, $M_d = 1.0$.

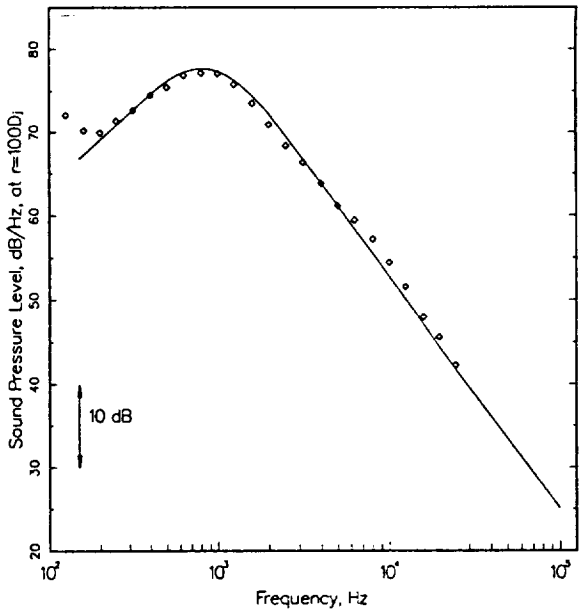

Figure 19. Comparison of the similarity spectrum of large turbulence structures/instability waves noise and subsonic jet noise measurement of Ahuja[18].
$M_j = 0.98$, $\chi = 160°$, $T_r/T_\infty = 1.0$.

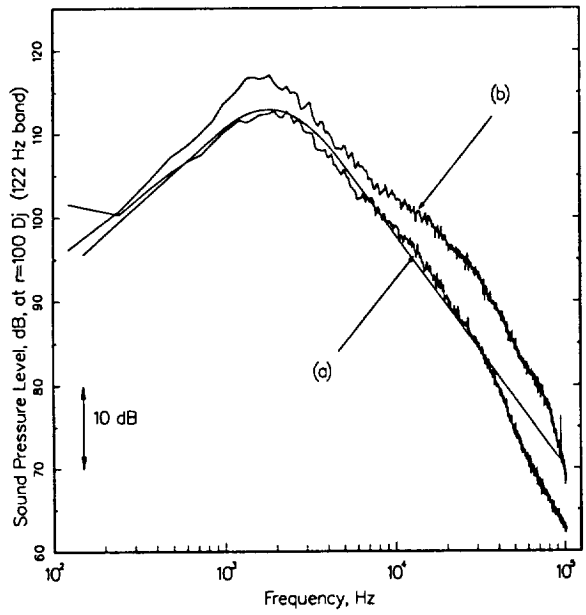

Figure 18. Experimental evidence of broadband amplification of large turbulence structures/instability waves noise in the presence of strong screech. $T_r/T_\infty = 1.0$, $\chi = 139.4°$, (a) $M_j = M_d = 1.49$, (b) $M_j = 1.49$, $M_d = 1.0$.

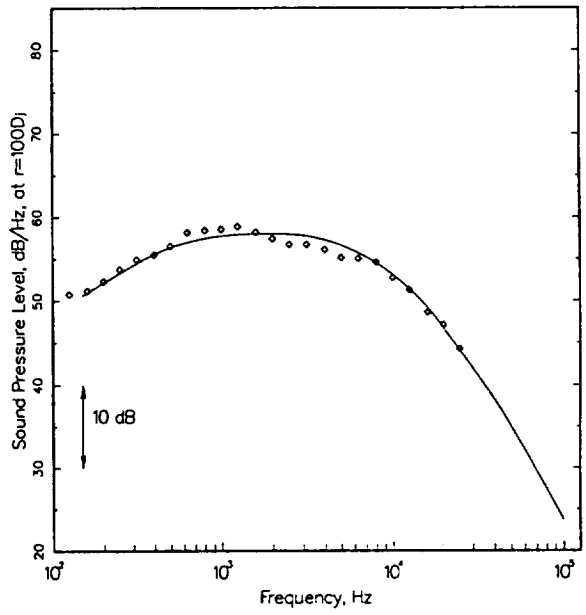

Figure 20. Comparison of the similarity spectrum of fine scale turbulence noise and subsonic jet noise measurement of Ahuja[18].
$M_j = 0.98$, $\chi = 90°$, $T_r/T_\infty = 1.0$.

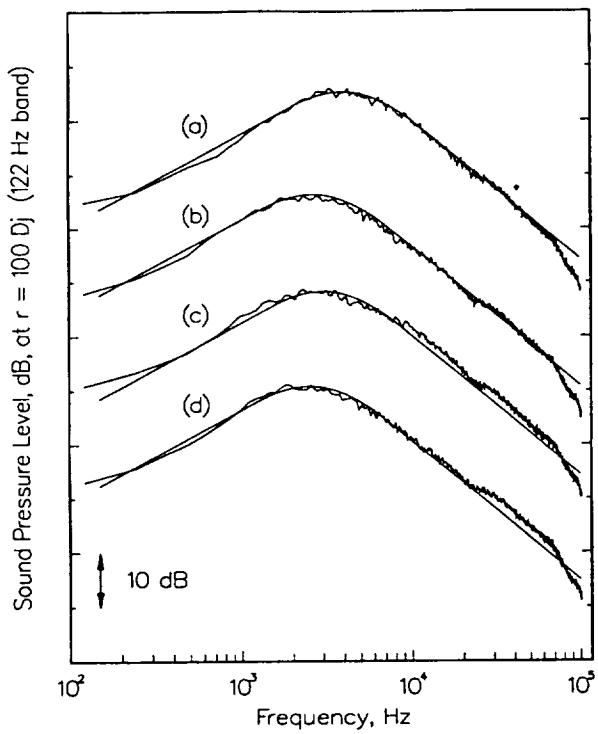

Figure 21. Comparison of the similarity spectrum of large turbulence structures/ instability waves noise and non-axisymmetric jet data.

(a) elliptic jet (aspec ratio 3) $M_j = M_d = 2.0$,
$T_r/T_\infty = 1.80$, $\chi = 130°$, $\phi = 90°$,$SPL_{\max} = 107$ dB,
(b) elliptic jet (aspec ratio 3) $M_j = M_d = 2.0$,
$T_r/T_\infty = 2.27$, $\chi = 130°$, $\phi = 0°$,$SPL_{\max} = 106$ dB,
(c) rectangular jet (a/r 7.6) $M_j = M_d = 2.0$,
$T_r/T_\infty = 2.26$, $\chi = 130°$, $\phi = 0°$,$SPL_{\max} = 106$ dB,
(d) rectangular jet (a/r 7.6) $M_j = M_d = 2.0$,
$T_r/T_\infty = 2.28$, $\chi = 130°$, $\phi = 90°$,$SPL_{\max} = 105$ dB.

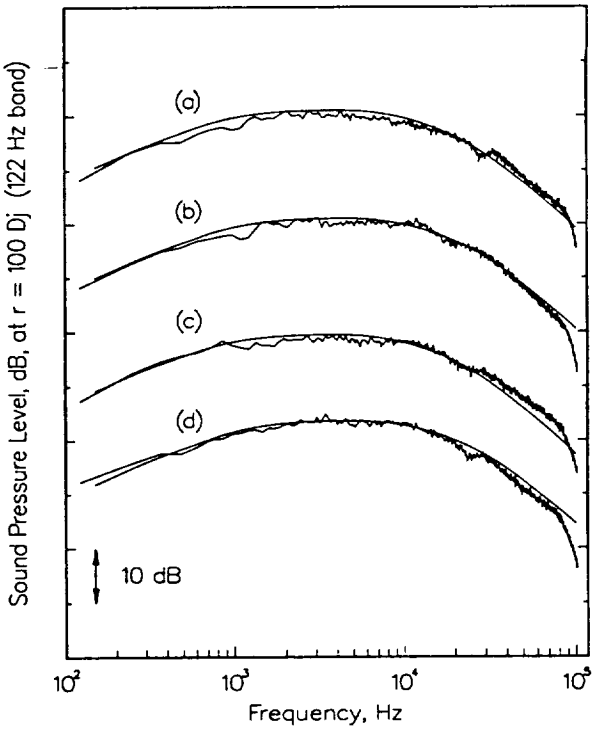

Figure 22. Comparison of the similarity spectrum of fine scale turbulence noise and non-axisymmetric jet data. (a) elliptic jet (aspec ratio 3) $M_j = M_d = 2.0$,
$T_r/T_\infty = 1.80$, $\chi = 108°$, $\phi = 0°$,$SPL_{\max} = 96$ dB,
(b) elliptic jet (aspec ratio 3) $M_j = M_d = 2.0$,
$T_r/T_\infty = 2.27$, $\chi = 89°$, $\phi = 90°$,$SPL_{\max} = 105$ dB,
(c) rectangular jet (a/r 7.6) $M_j = M_d = 2.0$,
$T_r/T_\infty = 2.26$, $\chi = 95°$, $\phi = 0°$,$SPL_{\max} = 99$ dB,
(d) rectangular jet (a/r 7.6) $M_j = M_d = 2.0$,
$T_r/T_\infty = 1.00$, $\chi = 89°$, $\phi = 90°$,$SPL_{\max} = 99$ dB.